Combustion and Flame 197 (2018) 78–87

Contents lists available at ScienceDirect

Combustion and Flame

journal homepage: www.elsevier.com/locate/combustflame

Studies of low temperature oxidation of n-pentane with nitric oxide addition in a jet stirred reactor

Hao Zhao[a,*], Lingnan Wu[a,b], Charles Patrick[c], Zunhua Zhang[a,d], Yacine Rezgui[e], Xueliang Yang[a], Gerard Wysocki[c], Yiguang Ju[a]

[a] Department of Mechanical and Aerospace Engineering, Princeton University, Princeton, NJ 08544-5263, USA
[b] Institute of Engineering Thermophysics, Chinese Academy of Sciences, Beijing 100190, China
[c] Department of Electrical Engineering, Princeton University, Princeton, NJ 08544-5263, USA
[d] School of Energy and Power Engineering, Wuhan University of Technology, Wuhan 430063, China
[e] University of Oum EI Bouaghi, Oum EI Bouaghi 15719, Algeria

ARTICLE INFO

Article history:
Received 27 April 2018
Revised 31 May 2018
Accepted 17 July 2018
Available online 7 August 2018

Keywords:
N-pentane
NO sensitization
Jet stirred reactor
Low temperature chemistry

ABSTRACT

The low temperature oxidation of n-pentane with nitric oxide (NO) addition has been investigated at 500–800 K in an atmospheric jet stirred reactor (JSR). The molar fraction of NO in the mixture is varied between 0 to 1070 ppm to study its chemical sensitization effect on low temperature oxidation of both fuel lean and rich n-pentane/oxygen mixtures. N-pentane, O_2, CO, CO_2, CH_2O, C_2H_4, CH_3CHO, NO, and NO_2 are quantified simultaneously, in-situ by using an electron impact molecular beam mass spectrometer (MBMS), a micro-gas chromatograph (μ-GC), and a sensitive mid-IR dual-modulation faraday rotation spectrometer (DM-FRS). The experimental results reveal that NO addition delays the onset temperature of low temperature oxidation of n-pentane between 550–650 K, but reduces the negative temperature coefficient (NTC) behavior in the NTC region (650–750 K) and dramatically shifts the onset of high temperature fuel oxidation to an intermediate temperature (750–800 K). A recently developed n-pentane/NO_x model by using Reaction Mechanism Generation (RMG) and a new n-pentane/NO_x model in the present work were used to predict the experimental results. The results show that the three distinct temperature-dependent characteristics of NO sensitized n-pentane oxidation are captured appropriately by these two models at both fuel rich and lean conditions, while the onset temperature of low temperature oxidation is not accurately predicted by these two models. It shows that the RMG model has a better prediction of the onset delay of n-pentane oxidation than Zhao's model, while Zhao's model performs better at NTC and intermediate temperature regions. Besides $RO_2 + NO$, additional fuel/NO_x reaction pathway, like $R + NO_2$, $RO + NO$, and $RO + NO_2$, and the interconversion reactions among NO, NO_2, and HONO may need to be further studied.

1. Introduction

Exhaust gas recirculation (EGR) is a strategy of reducing pollutants and controlling ignition and heat release rate in engines by diluting reactants with exhaust gases, containing species such as CO_2, H_2O, NO_x, etc. The ignition process in such a highly diluted mixture is very sensitive to the low temperature kinetics [1–4]. In addition to CO_2 and H_2O, NO is likely the most active species capable of altering ignition kinetics, especially at low and intermediate temperature [5]. Therefore, the NO sensitization effects on fuel oxidation, such as methane, 1-pentene, n-heptane, iso-octane, methanol, dimethyl ether (DME), and toluene, have been investigated in plug flow reactors, jet stirred reactors (JSR), and homogeneous charge compression ignition (HCCI) engines in experiments or simulations [4–14]. It has been shown that NO can accelerate or inhibit fuel oxidation depending on fuel types, temperature-pressure ranges, and NO concentrations.

Glaude et al. [4] performed a computational investigation of the mutual oxidation of NO and larger alkanes at low temperature, and found that mechanisms involving $NO + OH$ and $R + O_2$, where R is the fuel radical, contributes to the low temperature NO sensitization effect. Favarelli et al. [7] developed a general and detailed chemical kinetic model to investigate the interaction between NO and hydrocarbons, but had no exposure of the NO sensitization effect on the low temperature chemistry of hydrocarbons, especially on the NTC behavior. Dagaut et al. [9] studied the NO sensitization effect on DME oxidation in a JSR and de-

* Corresponding author.
E-mail address: haozhao@princeton.edu (H. Zhao).

https://doi.org/10.1016/j.combustflame.2018.07.014

veloped a detailed kinetic model to predict the experimental results. The results showed that DME oxidation was inhibited below 600 K due to $RO_2 + NO = RO + NO_2$, while promoted above 600 K due to $NO + HO_2 = NO_2 + OH$. Prabhu et al. [14] experimentally investigated the 1-pentene oxidation with 400 ppm NO addition in a flow reactor. The competing effect of NO was observed in experiment, but no kinetic modeling was conducted and the NO sensitization effect on the transition of the negative temperature coefficient (NTC) behavior was not examined. Therefore, there is limited experimental data of NO sensitization effect on low temperature fuel oxidations, especially accounting for the low temperature evolutions of intermediate species. Moreover, while the previous kinetic models may predict the fuel consumption profile reasonably well, the uncertainties in predicting intermediates species and NO_x in NO_x-fuel oxidation coupling remain large. Furthermore, the impact of NO sensitization on the NTC behavior was not well captured in experiments.

As one of the smallest alkanes which have rich low temperature reactivity, n-pentane has been investigated in experiments and simulations at both low and high temperatures [15–18]. A recent n-pentane model [17,18] shows a good agreement with experimental results. Therefore, n-pentane is chosen as a good target fuel for investigating the NO sensitization effect on low temperature oxidation.

The goal of the present study is to understand the NO sensitization effect on n-pentane oxidation in the low and intermediate temperature ranges. Special attention is paid to its impact on the onset of low temperature oxidation, the NTC effect, and the transition to high temperature ignition. The experiments of n-pentane oxidation with different amounts of NO additions (0, 300, and 1070 ppm) are performed at both lean and rich conditions at 500–800 K in an atmospheric pressure JSR. The mole fractions of n-pentane, O_2, CO, CO_2, CH_2O, C_2H_4, CH_3CHO, NO, and NO_2 are quantified simultaneously by using a molecular beam mass spectrometer (MBMS), a micro-gas chromatograph (μ-GC), and a sensitive mid-IR dual-modulation faraday rotation spectrometer (DM-FRS). A recently developed n-pentane/NO_x model using Reaction Mechanism Generator (RMG) [19] and a new n-pentane/NO_x model in the present work (Zhao's model) were used to predict the temperature evolutions of major and intermediate species and to capture the temperature-dependent NO sensitization characteristics.

2. Experimental methods and kinetic models

The experiments were performed in a fused silica JSR covered by a stainless-steel jacket with a regulated electrical resistance heating system. A 3-stage heating arrangement was employed to keep a uniform temperature distribution throughout the reactor. The jacket and the heating system were surrounded by insulating silica wool, allowing operating temperatures of up to 1300 K. The JSR is a sphere with an internal volume of 42 cm^3. In analogy to Dagaut's JSR design in [20,21], it has four nozzles of a 1 mm inner diameter at the center of the sphere to generate intense turbulence and homogenous mixing. This ensures homogeneity in concentration and residence time distributions inside the reactor. The volumetric flow rates of Ar, NO, N_2, and O_2 were regulated by mass flow controllers (MKS, 0.5% uncertainty), and liquid n-pentane was delivered by a syringe pump (Harvard Apparatus, PHD 22/2000) to a pre-vaporizer. A secondary nitrogen stream carried vaporized n-pentane gas from the vaporizer to the JSR entrance, and then mixed with the primary oxidizer stream (O_2/NO/Ar/N_2). The two streams are preheated by using separate heating arrangements. Specifically, lower power load was employed for the fuel stream to minimize the fuel pyrolysis in the preheating zone. Gas mixing time at the entrance of reactor is very short compared with the residence time inside the reactor (2–3%). The temperature profile inside the JSR was measured from 400 to 900 K by using the experimental gas mixture (n-pentane/O_2/NO/Ar/N_2) and is shown in Fig. S1 of the supplementary document. The temperature variation in the JSR was within ± 3 K. Samples of the reacting mixture were taken by sonic probes for the immediate analyses using MBMS, μ-GC, and mid-IR DM-FRS simultaneously for the cross-validation.

An electron-ionization MBMS with a mass resolution of $m/\Delta m = 900$ was employed to measure major combustion species at the exit of JSR, and the details of MBMS have been reported elsewhere [22–24]. Each important species was calibrated directly by flowing the mixture with known mole fractions in excessive N_2 and Ar. Oxygenated species (CH_2O and CH_3CHO) were calibrated using the mixtures prepared in a quartz vaporizer with a coflow of heated N_2 and Ar. Details of the species calibration were described elsewhere [22,23]. The measurement uncertainty was around 10-20%, which was mainly from the species calibration for MBMS and the electron impact (20 ± 1 eV) in MBMS. GC-TCD (Inficon 3000) was also used to identify and quantify stable combustion species (n-pentane, O_2, CH_2O, C_2H_4, CH_3CHO, CO and CO_2) from the exit of the reactor within a 5% uncertainty, and the details of μ-GC were described in [25–28]. An mid-IR DM-FRS system, developed at Princeton [29], was used to measure the NO concentration at the exit of the JSR within a 5% uncertainty. The mid-IR DM-FRS system targeted the $^{14}N^{16}O$ P(19/2)e doublet transition at 1842.946 cm^{-1} (major isotope) of NO. The pressure in the 15-cm triple pass gas cell was stabilized at 80 torr with a flow rate of 56 sccm. Modulations of both the laser current and the applied magnetic field provided laser intensity independent and etalon-free measurements. The resulting sidebands from the modulation were demodulated using a lock-in amplifier to reach a noise-equivalent angle of 10^{-8} rad·$Hz^{-1/2}$. The NO detection limit of the mid-IR DM-FRS system is ~1 ppb. More details of the diagnostic system can be found elsewhere [29]. The present experiment has a maximum uncertainty of 20%, which is mainly from the direct species calibration for MBMS and the electron impact (20eV ± 1 eV) in MBMS. For gas phase species calibrations, the uncertainty is around 10%; while for liquid samples calibrations (CH_2O and CH_3CHO), the data has an uncertainty of 20%. In addition, the sample quantification in μ-GC and DM-FRS has an uncertainty within 5%.

The experiments were performed for both fuel lean and rich conditions ($\varphi = 0.5$ and 1.33) with different amounts of NO additions at 500-800 K and 1 atm. The experimental conditions are shown in Table 1. Temperature of the feed gases entering the reactor is 295 K. The inlet volume flow rate is fixed at 969 ml/min at 295 K, as such, the residence time in the reactor varies with reactor temperature (T) through

$$\tau = (V/\upsilon) * T_0/T,$$

where, V is the volume of the JSR, υ is the inlet volume flow rate at room temperature, T_0 is the room temperature (295 K). Reactants are mixed based on mole fraction percentage. The residence time was regulated with temperature to be comparable with the calculated characteristic reaction time scale of n-pentane low temperature oxidation in Chemkin [30]. Species measurements were repeated 2-3 times at every experimental condition with repeatability uncertainty below 2%.

A recently developed RMG n-pentane/NO_x model [19] and a new n-pentane/NO_x model in the present work (Zhao's model) were used to predict the experimental results. The RMG model was obtained by relying on Bugler's n-pentane kinetic framework [17], the RMG NO_x library, and additional n-pentane/NO_x coupling reaction subsets generated using the open-source automated Reaction Mechanism Generation software v2.1.0 [31,32]. While generating this model, particular attention was given to reactions of NO/NO_2 affecting the concentrations of oxy (RO) and peroxy (RO_2) radicals

Table 1
Experimental conditions.

Case	Equivalence ratio	N-C_5H_{12} (%)	O_2 (%)	Ar (%)	N_2 (%)	NO (ppm)	Residence time (s)	Temperature range (K)
1	0.5	1	16	5	78	0	1.53–0.96	500–800
2	0.5	1	16	1.370	81.6	300	1.53–0.96	500–800
3	0.5	1	16	4.893	78	1070	1.53–0.96	500–800
4	1.33	1	6	5	88	0	1.53–0.96	500–800
5	1.33	1	6	1.370	91.6	300	1.53–0.96	500–800

Table 2
Modified rate coefficients of $RO_2 + NO$, $NO_2 + CH_3$, $NO_2 + HO_2$, $NO + OH$, and $NO + HO_2$[a].

Reaction	A (cm^3/mol/s)	n	Ea (cal/mol)	A factor modification	Model uncertainty	Reference
$C_5H_{11}O_2$-1 + NO = $C_5H_{11}O$-1 + NO_2	6.325E + 13	0	1058	–	N/A	[40][b]
$C_5H_{11}O_2$-2 + NO = $C_5H_{11}O$-2 + NO_2	6.325E + 13	0	1058	–	N/A	[40][b]
$C_5H_{11}O_2$-3 + NO = $C_5H_{11}O$-3 + NO_2	6.325E + 13	0	1058	–	N/A	[40][b]
$NO_2 + CH_3 = NO + CH_3O$	1.400E + 14	0	0	x10	N/A	[41]
$NO_2 + HO_2 = HONO + O_2$	1.446E + 10	0	0	x0.2	N/A	[42]
$NO + HO_2 = NO_2 + OH$	5.00e + 12	0	−477	x2.27	N/A	[33]
NO + OH + M = HONO + M	5.97E + 12	−0.05	−721.00	x3	x5	[37]
	Low/1.524E + 24	−2.51	−67.60	x3		

[a] For the modified Arrhenius form $k = A \cdot T^n \cdot e^{Ea/RT}$, where, A is the pre-exponential factor, n is the reaction order, Ea is the activation energy, T is the reaction temperature, and R is the gas constant.
[b] Analogical with $CH_3O_2 + NO = CH_3O + NO_2$ from [40] and updated based on the experiment in this study.

in the system. An additional NO_x sub-mechanism was built based on the kinetic data reported in the seminal review by Dean and Bozzelli [33] with relevant updates and additions from the RMG NO_x library. Details of the RMG model is elsewhere [19].

The present model shares the same n-pentane kinetic framework [17] with an independently developed NO_x sub-mechanism by Princeton, and additional n-pentane/NO_x coupling reaction subsets. Previous experiments showed that this n-pentane mechanism predicted the major and intermediate species temperature evolution profiles of n-pentane oxidation at both low and high temperatures successfully [17,18]. The whole nitrogen sub-mechanism involves around 21 species and 240 reactions. The base rates were mainly extracted from the theoretical work of Glarborg et al. [34,35] with relevant updates. The latter includes the following pathways: thermal NO (mainly based on Bromly et al. [36]), NO_2 and HONO subsets (mainly based on Muller et al. [37]), N_2O, NH, NH_2, NH_3 and HHN subsets (mainly based on Klippenstein et al. [38]), NO_3 and HNO_3 subsets (mainly based on Bromly et al. [36] and Muller et al. [37]), N_2H_2, N_2H_3, and N_2H_4 subsets (mainly based on A.M. Dean and J.W. Bozzelli [33]), and some other updated rates from NIST database. The training experimental data sets were mainly from Mueller and Amarno's flow reactor results ($H_2 + NO_x$ and $CH_4 + NO_x$) [37,39] and Dagaut's JSR results (DME + NO_x) [9]. The coupling reaction rates between the n-pentane mechanism and the NO_x sub-mechanism, like $RH + NO_2$, $RO_2 + NO$, $RO + NO$, $R + NO_2$, etc., were determined by analogy with the n-heptane/NO_x coupling rates in Glaude et al. [4] and Andrae et al. [13]. The rate coefficients of $RO_2 + NO$, $CH_3 + NO_2$, $NO_2 + HO_2$, $NO + OH$, and $NO + HO_2$ were updated to capture the temperature-dependent NO sensitization effects based on the experimental results in this paper, and were shown in Table 2. Simulation was performed in the perfectly stirred reactor module of Chemkin software by using a transient solver [30].

3. Results and discussion

Figure 1 depicts the mole fraction of n-pentane versus the gas temperature at both fuel rich and lean conditions ($\varphi = 0.5$ and 1.33) without NO addition. The low temperature oxidation of n-pentane is clearly observed in the experiment, and the n-pentane mole fractions measured in MBMS and μ-GC agree within 10%. Bugler's n-pentane mechanism predicts the low temperature oxidation window at fuel lean condition favorably, while slightly under-

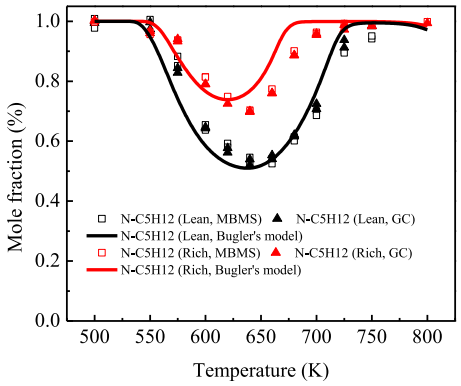

Fig. 1. Temperature evolution of the mole fraction of n-pentane at the fuel rich and lean conditions ($\varphi = 0.5$ and 1.33) without NO addition.

predicts the consumption of n-pentane at fuel rich condition. In addition, the onsets of the oxidation at both fuel lean and rich conditions are captured in the model simulation successfully. The mole fraction profiles of the main products (CO and CO_2) and intermediates (CH_2O, CH_3CHO) are plotted in Figs. S2–S4 in the supplementary document. It is seen that the temperature evolutions of these species are generally well-predicted in Bugler's n-pentane mechanism, except for CH_3CHO. It verifies the motivation to use n-pentane as a target fuel to investigate the NO sensitization effect. In this work, the present n-pentane/NO_x model (Zhao's model) and the RMG model, consisting of Bugler's n-pentane mechanism with different NO_x reaction subsets, are used for the simulation.

The mole fraction profiles of n-pentane at the lean conditions ($\varphi = 0.5$) with different amounts of NO additions (0, 300, and 1070 ppm) are shown in Fig. 2, respectively. In the experiment, it is clearly seen that NO has a significant effect on n-pentane oxidation. Specifically, NO exhibits different sensitization effects in the three different temperature windows. Firstly, NO inhibits the low temperature oxidation and delays its onset temperature at 550–650 K. Secondly, NO weakens the NTC effect in the NTC region (650–750 K). Thirdly, NO addition accelerates high temperature oxidation and shifts it significantly to lower temperature (750–800 K). It is seen that the onset temperature of low temperature oxidation of n-pentane is delayed, respectively, from 550 K (case 1 without NO addition) to 585 K (case 2 with 300 ppm NO addition) and 620 K (case 3 with 1070 ppm NO addition), indicating a strong in-

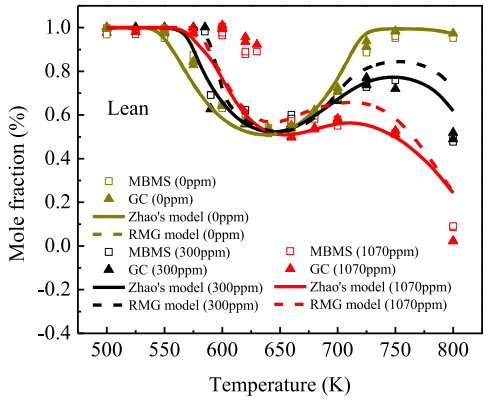

Fig. 2. Temperature evolution of the mole fraction of n-pentane at the fuel lean conditions ($\varphi = 0.5$) with different amounts of NO additions (0, 300, and 1070 ppm).

hibiting effect of NO on n-pentane oxidation in the low temperature oxidation window. However, with the increase of temperature to the NTC region, the NTC behavior of n-pentane becomes significantly weaker with the increase of NO concentrations, indicating that NO addition promotes low temperature oxidation reactivity and reduces the NTC effect kinetically. Moreover, without NO addition, the high temperature oxidation of n-pentane starts at temperatures above 800 K. However, with 300 ppm NO addition, the high temperature oxidation is accelerated to a lower temperature of around 750 K. Furthermore, with the increase of NO addition to 1070 ppm, the onset of high temperature oxidation is further shifted to lower temperature and nearly all of the fuel is oxidized at 800 K.

In the model prediction, it is seen that Zhao's model and the RMG model have the same prediction of n-pentane oxidation at the condition without NO addition as expected since they are both based on the modified n-pentane model [17]. Moreover, both Zhao's model and the RMG model have captured the three temperature-dependent sensitization characteristics of NO reasonably well and exhibited the onset delay of the low temperature oxidation with NO addition. Furthermore, the RMG model has a better prediction of the onset delay of n-pentane oxidation than Zhao's model, while Zhao's model performs better at NTC and intermediate temperature regions. However, both models fail to predict the onset delay with 1070 NO additions precisely. It implies that there is still a large uncertainty in the n-pentane/NO_x coupling reactions of these two models, especially at the oxidation initiation region.

To explain the NO sensitization effect, the pathway analyses of n-pentane were, respectively, performed at 610 K (low temperature region), 680 K (NTC region), and 780 K (intermediate temperature region) at the fuel lean condition with 1070 ppm NO addition by using Zhao's model, and the results are shown in Fig. 3(a)–(c). In the low temperature oxidation region, Fig. 3(a) shows that there are three reaction channels for RO_2 consumption,

$$RO_2 = QOOH \quad (R1)$$

$$RO_2 + NO = RO + NO_2 \quad (R2)$$

$$RO_2 + M = C_5H_{10} + HO_2 + M \quad (R3)$$

Note that reaction R_1 is part of the typical low temperature oxidation channel for OH radical production. Reaction R_2 is a alternative RO_2 consumption channel with NO and produces three isomers, RO-1 ($C_5H_{11}O$-1), RO-2 ($C_5H_{11}O$-2), and RO-3 ($C_5H_{11}O$-3). Reaction R_3 is a decomposition channel to form HO_2. Since RO and

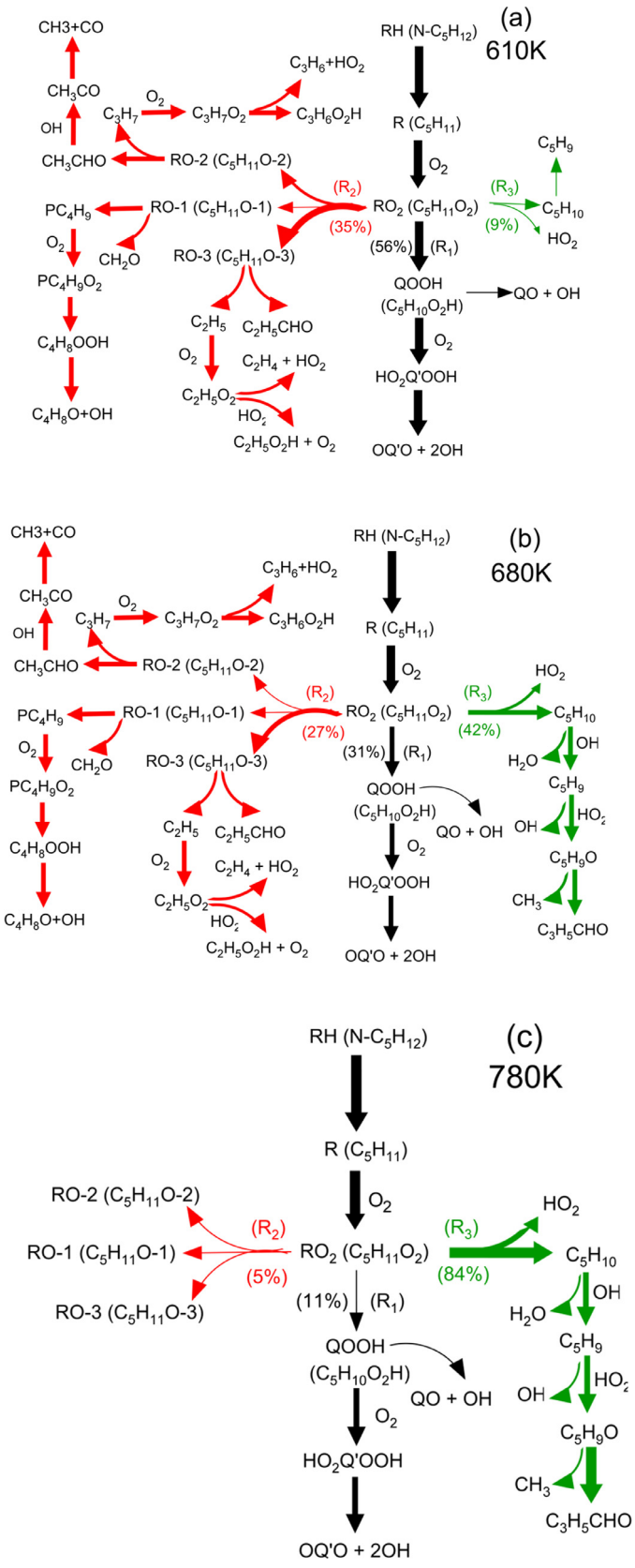

Fig. 3. (a)-(c) Pathway analysis of n-pentane at 610, 680, and 780 K, respectively, in the fuel lean condition ($\varphi = 0.5$) with 1070 ppm NO addition by using Zhao's model.

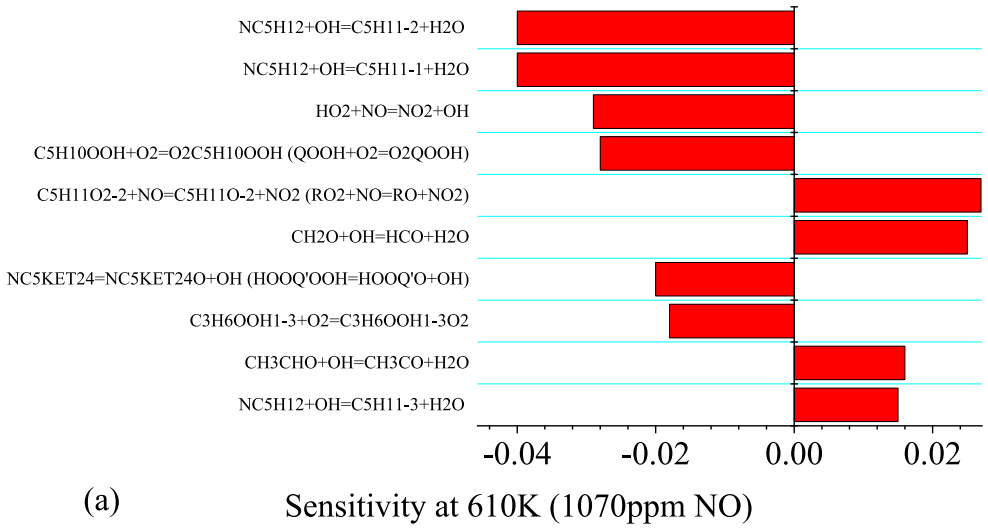

(a) Sensitivity at 610K (1070ppm NO)

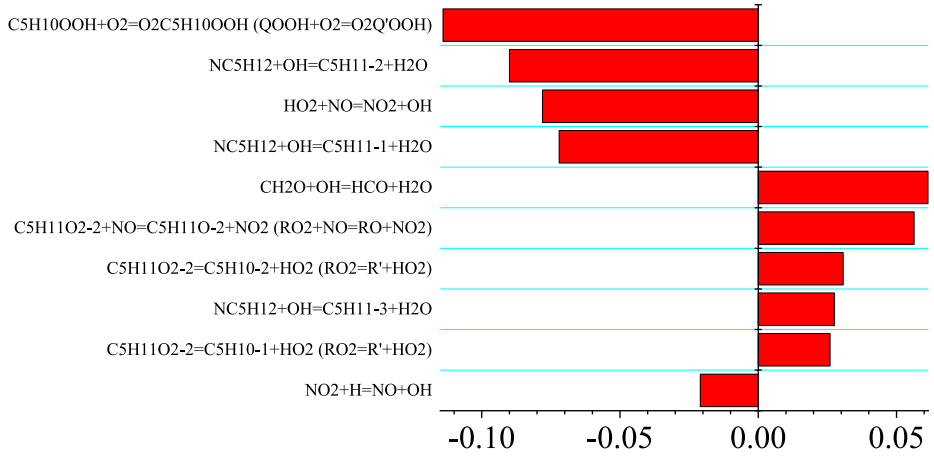

(b) Sensitivity at 680K (1070ppm NO)

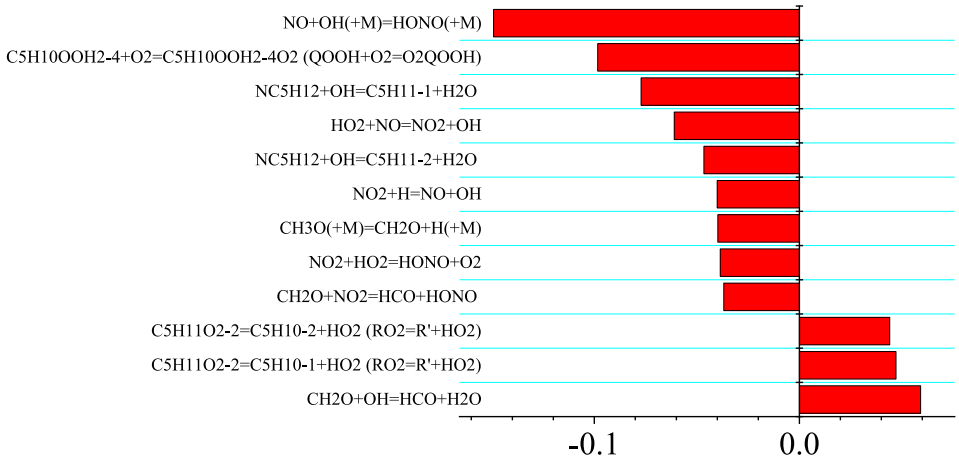

(c) Sensitivity at 780K (1070ppm NO)

Fig. 4. Sensitivity analysis of n-pentane at 610, 680, and 780 K, respectively, in the fuel lean condition ($\varphi = 0.5$) with 1070 ppm NO addition by using Zhao's model.

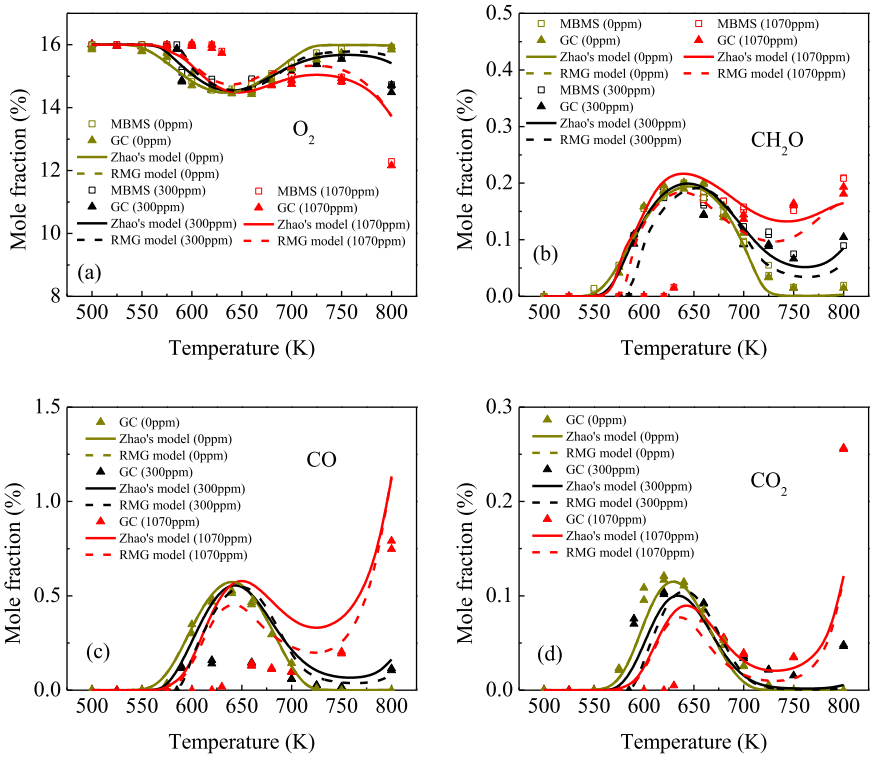

Fig. 5. Temperature evolutions of the concentrations of O_2, CH_2O, CO, and CO_2 at the fuel lean conditions ($\varphi = 0.5$) with different amounts of NO additions (0, 300, and 1070 ppm).

HO_2 are much less reactive than OH in the low temperature region, reaction channels R_2 and R_3 inhibit the low temperature oxidation.

As such, without NO addition, the low temperature oxidation of n-pentane proceeds through reaction channel R_1 to form QOOH and a second oxygen addition will lead to O_2QOOH and the subsequent formation of two OH radicals. With NO addition, reaction channel R_2 dominates the consumption of RO_2 and reduces the formation of QOOH, thus slowing down the reactivity. Moreover, in this temperature range, NO consumes OH quickly by forming a relative stable species HONO through

$$NO + OH + M = HONO + M \quad (R4)$$

Therefore, reaction R_4 further reduces the low temperature reactivity. As such, the inhibiting effect of NO on the onset of the low temperature fuel oxidation is mainly through the reaction channels of R_2–R_4.

In the NTC region, reaction channels of R_1–R_3 are all important, as shown in Fig. 3(b). It is seen that HO_2 and CH_3 are produced significantly via the pathways of reaction channel R_2 and R_3. At this temperature, HO_2 can react with NO to produce active radical OH through the following reaction channels,

$$HO_2 + NO = OH + NO_2 \quad (R5)$$

$$NO_2 + HO_2 = HONO + O_2 \quad (R6)$$

$$HONO + M = OH + NO + M \quad (R-4)$$

CH_3 also reacts with NO_2 to regenerate H and OH radicals through reactions,

$$NO_2 + CH_3 = CH_3O + NO \quad (R7)$$

$$CH_3O + M = CH_2O + H + M \quad (R8)$$

$$CH_2O + NO_2 = HCO + HONO \quad (R9)$$

$$HONO + M = OH + NO + M \quad (R-4)$$

Therefore, different from the NO inhibiting role at 550–650 K, in the NTC region, reaction channel R_2 and R_3 now play a promoting effect in producing OH and H radicals to increase the reactivity and reduce the NTC effect. It is well-known that the NTC effect is caused by the acceleration of RO_2 decomposition and QOOH dissociation at higher temperature [6,16]. However, in the NTC region, NO addition promotes fuel oxidation through reaction channel R_2 and other reactions discussed above. This explains the weakening NTC effect with NO addition. Note that at higher NO addition (1070 ppm), the NO sensitization effect becomes so large that the NTC behavior almost disappears.

With a further increase of temperature above 750 K, Fig. 3(c) shows that the reaction channel R_3 dominates the RO_2 decomposition pathways. HO_2 and CH_3 react much faster with NO and NO_2, respectively, to regenerate active radicals, OH and H. Therefore, NO dramatically promotes high temperature oxidation through reactions R_3–R_9, causing a dramatic shift of high temperature oxidation to lower temperature.

The sensitivity analyses of the n-pentane mole fraction at the fuel lean condition with 1070 ppm NO addition were also performed at 610, 680, and 780 K by using Zhao's model in Fig. 4 to confirm the discussion in the pathway analyses. At 610 K and 680 K, the most sensitive reactions are the H abstraction reactions of n-pentane, the competing reactions of QOOH decomposition and QOOH + O_2, reaction R_2, reaction R_5, and the reaction $CH_2O + OH = HCO + H_2O$, which are involved in reaction pathways through reaction channels R_1 and R_2. At 780 K, reactions R_3–R_6 through reaction channel R_3 become more sensitive, which corresponds to the pathway analysis in Fig. 3(c).

The mole fraction profiles of O_2, CO, CO_2, CH_2O, C_2H_4, CH_3CHO, NO and NO_2 at the fuel lean conditions are shown in Figs. 5 and 6,

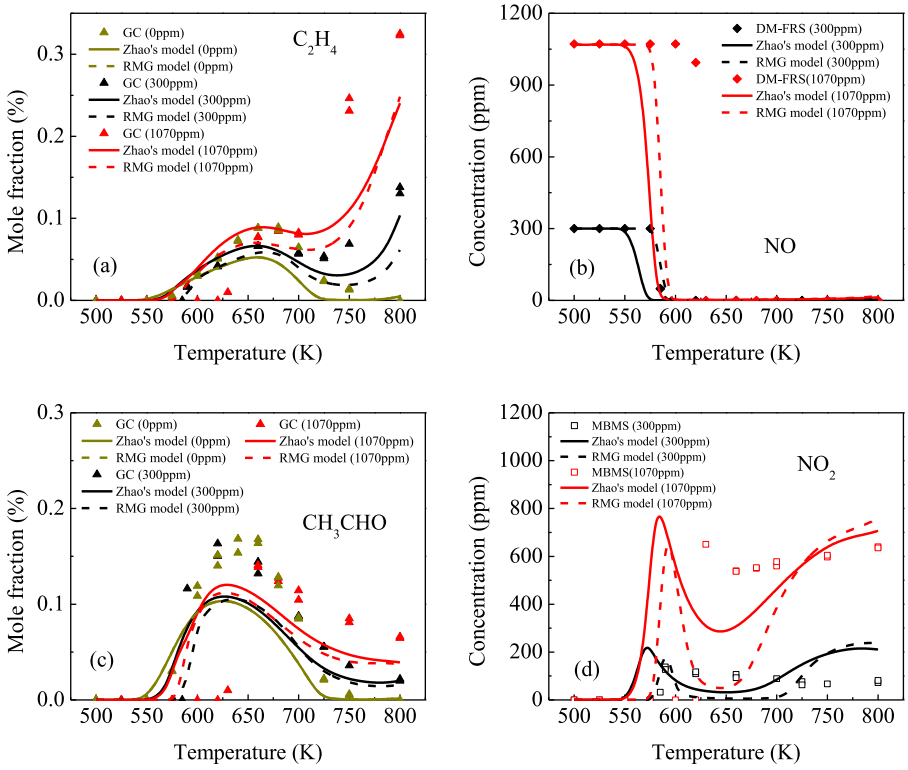

Fig. 6. Temperature evolutions of the mole fractions of C_2H_4, NO, CH_3CHO, and NO_2 at the fuel lean conditions ($\varphi = 0.5$) with different amounts of NO additions (0, 300, and 1070 ppm).

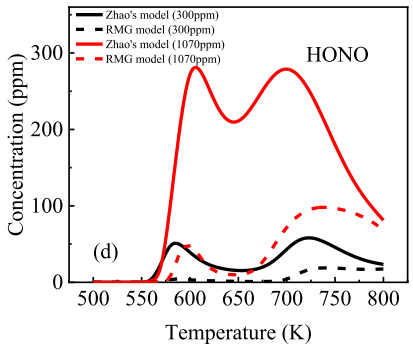

Fig. 7. Temperature evolutions of the predicted mole fraction of HONO at the fuel lean conditions ($\varphi = 0.5$) with different amounts of NO additions (300 and 1070 ppm).

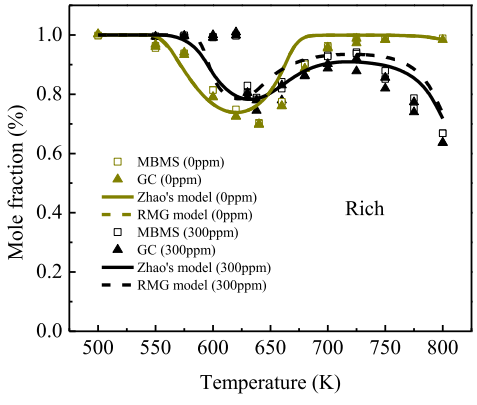

Fig. 8. Temperature evolution of the mole fraction of n-pentane at the fuel rich conditions ($\varphi = 1.33$) with and without 300 ppm NO additions.

respectively. When low temperature oxidation of n-pentane starts, NO is dramatically consumed to produce NO_2 and HONO through reactions R_2 and R_4, respectively, and there is no observation of NO signal in the mid-IR DM-FRS system at higher temperatures. Moreover, the RMG model has a better performance on predicting NO mole fraction profile than Zhao's model, which is corresponding with the model simulations on predicting the onset delay of low temperature oxidation in Fig. 2. Both Zhao's model and the RMG model predict the major products and intermediates reasonably well. However, because of the mis-prediction of onset delay of oxidation with NO addition, the mole fraction profiles of the species at 600–640 K are not appropriately captured. Additionally, both models mis-predict the temperature evolutions of NO_2 with 1070 NO additions. Specifically, the RMG model shows an excessive conversion of NO_2 to HONO at 600–700 K. Therefore, the present models need to be improved to predict NO_2 concentration accurately, especially in the coupling reactions between $RH + NO_2$, $R + NO_2$, $RO_2 + NO$, $RO + NO$, and $RO + NO_2$,. Both Zhao's model and the RMG model mainly focus on the coupling reactions of $RO_2 + NO$ with optimization, while the other four sets of n-pentane/NO_x coupling reactions are still lacking of elaborate study. Furthermore, models also show some discrepancies in predicting O_2, CO and CO_2 mole fractions with NO addition at 800 K. Therefore, according to the sensitivity analysis of CO_2 at 800 K using Zhao's model, the interaction reactions between CO/CO_2 and NO_x, especially the reaction,

$$CO + NO_2 = CO_2 + NO \quad \text{(R10)}$$

might need to be updated to capture the correct CO and CO_2 temperature evolutions.

The predicted HONO mole fraction profiles by using Zhao's model and the RMG model at the lean conditions are depicted in Fig. 7 to verify the pathway analyses in Fig. 3. It is seen that HONO

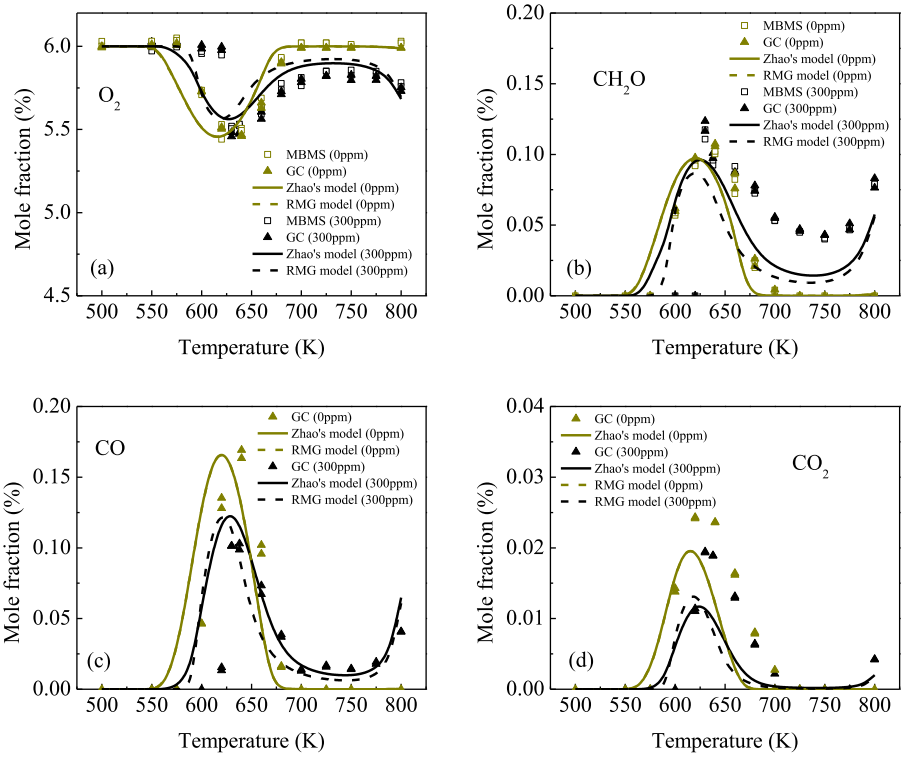

Fig. 9. Temperature evolutions of the concentrations of O_2, CH_2O, CO, and CO_2 at the fuel rich conditions ($\varphi = 1.33$) with and without 300 ppm NO addition.

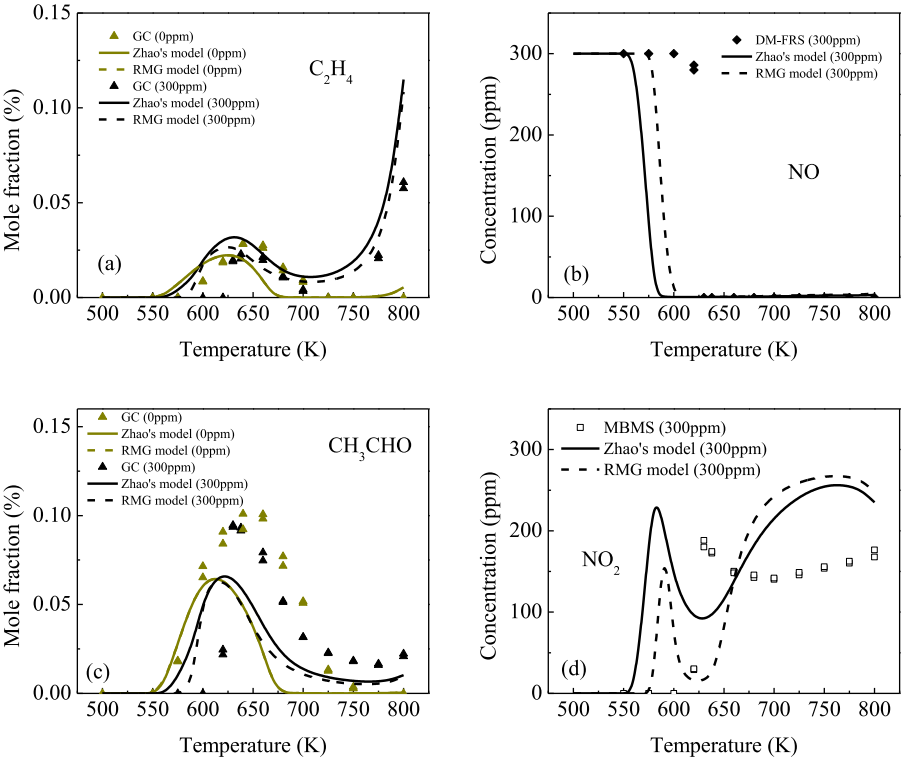

Fig. 10. Temperature evolutions of the concentrations of C_2H_4, NO, CH_3CHO, and NO_2 at the fuel rich conditions ($\varphi = 1.33$) with and without 300 ppm NO addition.

is produced in the low temperature region, while decomposed dramatically through reaction R_4 in the intermediate temperature region. The RMG model has a less prediction of HONO mole fraction than Zhao's model both at the lean conditions with 1070 and 300 ppm NO additions. That is because CH_3NO_2 is included in the RMG model, which is formed from $CH_3 + NO_2$ and competes with HONO production, while it is not considered in Zhao's model. Experimental quantification of HONO and CH_3NO_2 is needed in the future alkane/NO_x kinetic study to validate the pathways of nitrogen containing species in models.

The temperature evolutions of n-pentane at the fuel rich conditions ($\varphi = 1.33$) with and without 300 ppm NO additions are shown

in Fig. 8. Similar to the fuel lean case, both models have captured the three temperature-dependent NO sensitization characteristics at the rich case: the delay of the onset temperature of low temperature oxidation, the weakening effect of NTC behavior in the NTC region, and the acceleration of high temperature oxidation in the intermediate temperature region. The major pathways of n-pentane oxidation in the three temperature regions at the fuel rich condition with 300 ppm NO addition are also similar to that at the lean condition. Nevertheless, there are more CH_3 and H radicals formed in the fuel rich case than that in the lean case. As such, reaction R_7 becomes more evident than reaction R_5 in accelerating reaction channels R_2 and R_3.

Figures 9 and 10 depict the concentrations of O_2, CO, CO_2, CH_2O, C_2H_4, CH_3CHO, NO, and NO_2 versus the mixture temperature at the fuel rich conditions with and without NO addition. Both models predict the key intermediates and products well from 500 K to 800 K. Nevertheless, they still fail to accurately capture the NO_2 concentration profile. In the simulation using Zhao's model, NO_2 concentration increases significantly at 575–600 K due to the NO_2 production from reaction R_2. At 600–650 K, reactions R_6 and R_7 increase significantly and NO_2 concentration dramatically decreases. Above 650 K, HONO begins to decompose to NO through (R_{-4}), and the interconversion between NO and NO_2 becomes very fast, leading to an increase of NO_2 from NO. However, in the experiment, NO_2 concentration decreases and increases slowly at 630-660 K and 660–800 K, respectively. It implies a large uncertainty either in the n-pentane/NO_x coupling reactions or interconversion reactions among NO, NO_2, and HONO. Therefore, HONO needs to be quantified in the future study to analyze the model uncertainty.

4. Conclusion

The NO sensitization effect of n-pentane low temperature oxidation was investigated at both fuel lean and rich conditions with different levels of NO additions in an atmospheric pressure JSR with different diagnostic methods. Experimental results show that NO has a significant kinetic effect on low temperature n-pentane oxidation. Specifically, NO exhibits three different sensitization effects in three different temperature windows. Firstly, NO inhibits low temperature oxidation and delays the onset temperature of the low temperature oxidation window (550–650 K). Secondly, NO promotes fuel reactivity and reduces the NTC effect between 650–750 K. The NTC behavior is almost disappeared with 1070 ppm or higher NO addition. Thirdly, NO dramatically accelerates high temperature oxidation and shifts the high temperature fuel oxidation from above 800 K to 750 K. A recently developed RMG n-pentane/NO_x model and the present n-pentane/NO_x model (Zhao's model) were used to predict temperature evolutions of major and intermediate species.

Pathway analyses reveal that three reaction channels of RO_2 consumption, reactions R_1–R_3, dominate the n-pentane/NO kinetics. At 550-650 K, with NO addition, reaction channel R_2 and R_3 inhibits n-pentane oxidation, and reaction R_4 further reduces the reactivity. However, in the NTC region, reaction channel R_2 and R_3 promotes n-pentane oxidation and weakens the NTC behavior, and the NTC phenomenon almost disappears at higher NO addition (1070 ppm). In the intermediate temperature region, NO dramatically promotes high temperature oxidation through reaction channel R_3, causing a shift of high temperature oxidation to lower temperature.

The results show that the experiments and the model predictions agree reasonably well at both fuel rich and lean conditions. The RMG model has a better prediction of the onset delay of n-pentane oxidation than Zhao's model, while Zhao's model performs better at NTC and intermediate temperature regions. Moreover, both models fail to predict the onset delay with 1070 NO additions precisely. Both models mis-predict the NO_2 profile at the fuel lean and rich cases. Therefore, additional fuel/NO_x reaction pathways, like $R + NO_2$, $RO + NO$, and $RO + NO_2$, and the interconversion reactions among NO, NO_2, and HONO may need to be further studied.

Acknowledgments

This work was supported by NSF CBET-1507358 research grant and the Princeton Environmental Institute (PEI)-Andlinger Center for Innovative Research Awards in Energy and the Environment.

Supplementary materials

Supplementary material associated with this article can be found, in the online version, at doi:10.1016/j.combustflame.2018.07.014. Any updates of Zhao's n-pentane/NO_x model and the RMG n-pentane/NO_x model can be tracked from http://engine.princeton.edu/mechanism.html.

References

[1] J.E. Dec, Advanced compression-ignition engines—understanding the in-cylinder processes, Proc. Combust. Inst. 32 (2009) 2727–2742.
[2] V. Knop, S. Jay, Latest developments in gasoline auto-ignition modeling applied to an optical CAI (Tm) engine, Oil Gas Sci. Technol. 61 (2006) 121–137.
[3] J.T. Kashdan, J.F. Papagni, LIF imaging of auto-ignition and combustion in a direct injection diesel-fuelled HCCI engine, SAE, 2005 2005-01-3739.
[4] P.A. Glaude, N. Marinov, Y. Koshiishi, et al., Kinetic modeling of the mutual oxidation of no and larger alkanes at low temperature, Energy Fuels 19 (2005) 1839–1849.
[5] G. Moréac, P. Dagaut, J.F. Roesler, M. Cathonnet, Nitric oxide interactions with hydrocarbon oxidation in a jet-stirred reactor at 10 atm, Proc. Combust. Inst 2 (2002) 240–251.
[6] C.L. Rasmussen, A.E. Rasmussen, P. Glarborg, Sensitizing effects of NO_x on CH_4 oxidation at high pressure, Combust. Flame 154 (2008) 529–545.
[7] T. Faravelli, A. Frassoldati, E. Ranzi, Kinetic modeling of the interactions between NO and hydrocarbons in the oxidation of hydrocarbons at low temperatures, Combust. Flame 132 (2003) 188–207.
[8] M.U. Alzueta, J. Muro, R. Bibao, P. Glarborg, Oxidation of dimethyl ether and its interaction with nitrogen oxides, Israel J. Chem. 39 (1999) 73–86.
[9] P. Dagaut, J. Luche, et al., The low temperature oxidation of DME and mutual sensitization of the oxidation of DME and nitric oxide: Experimental and detailed kinetic modeling, Combust. Sci. Tech 165 (2001) 61–84.
[10] J.M. Anderlohr, R. Bounaceur, A. Pires Da Cruz, F. Battin-Leclerc, Modeling of autoignition and NO sensitization for the oxidation of IC engine surrogate fuels, Combust. Flame 156 (2009) 505–521.
[11] A. Dubreuil, F. Foucher, et al., HCCI combustion: Effect of NO in EGR, Proc. Combust. Inst. 31 (2007) 2879–2886.
[12] F. Contino, F. Foucher, P. Dagaut, et al., Experimental and numerical analysis of nitric oxide effect on the ignition of iso-octane in a single cylinder HCCI engine, Combust. Flame 160 (2013) 1476–1483.
[13] J.C.G. Andrae, Kinetic modeling of the influence of NO on the combustion phasing of gasoline surrogate fuels in an HCCI engine, Energy Fuels 27 (2013) 7098–7107.
[14] S.K. Prabhu, R.K. Bhat, et al., 1-Pentene oxidation and its interaction with nitric oxide in the low and negative temperature coefficient regions, Combust. Flame 104 (1996) 377–390.
[15] M. Ribaucour, R. MinettiL., R. Sochet, Autoignition of n-pentane and 1-pentene: Experimental data and kinetic modeling, Symp. (Int.) Combust. 27 (1998) 345–351.
[16] J. Bugler, K.P. Somers, E.J. Silke, H.J. Curran, Revisiting the kinetics and thermodynamics of the low-temperature oxidation pathways of alkanes: a case study of the three pentane isomers, J. Phys. Chem. A 119 (2015) 7510–7527.
[17] J. Bugler, A. Rodriguez, et al., An experimental and modeling study of n-pentane oxidation in two jet-stirred reactors: The importance of pressure-dependent kinetics and new reaction pathways, Proc. Combust. Inst. 36 (2017) 441–448.
[18] A. Rodriguez, O. Herbinet, et al., Measuring hydroperoxide chain-branching agents during n -pentane low-temperature oxidation, Proc. Combust. Inst. 36 (2017) 333–342.
[19] H. Zhao, A. Dana, Z. Zhang, W. Green, Y. Ju, Experimental and modeling study of the mutual oxidation of n-pentane and nitrogen dioxide at low and high temperatures in a jet stirred reactor, Energy (2018) Under review.
[20] P. Dagaut, M Cathonnet, J.P. Rouan, et al., A jet-stirred reactor for kinetic studies of homogeneous gas-phase reactions at pressures up to ten atmospheres (~1MPa), J. Phys. E Sci. Instrum 19 (1986) 207–209.
[21] T. Zhang, H. Zhao, Y. Ju., Numerical studies of residence time distributions of a novel inwardly off-center shearing jet-stirred reactor (IOS-JSR), AIAA J. (2018) In press.

[22] H. Zhao, X. Yang, Y Ju, Kinetic studies of ozone assisted low temperature oxidation of dimethyl ether in a flow reactor using molecular-beam mass spectrometry, Combust. Flame 173 (2016) 187–194.
[23] D. Felsmann, H. Zhao, Q. Wang, et al., Contributions to improving small ester combustion chemistry: Theory, model and experiments, Proc. Combust. Inst. 36 (2017) 543–551.
[24] L. Tran, J. Pieper, H. Carstensen, et al., Experimental and kinetic modeling study of diethyl ether flames, Proc. Combust. Inst. 36 (2017) 1165–1173.
[25] H. Zhao, J. Fu, F.M. Haas, Y. Ju, Effect of prompt dissociation of formyl radical on 1, 3, 5-trioxane and CH_2O laminar flame speeds with CO_2 dilution at elevated pressure, Combust. Flame 183 (2017) 253–260.
[26] A. Rousso, S. Yang, et al., Low temperature oxidation and pyrolysis of n-heptane in nanosecond-pulsed plasma discharges, Proc. Combust. Inst. 36 (2017) 4105–4112.
[27] H. Zhao, J. Fu, Y. Ju, Effect of "prompt" dissociation of formyl radical on high temperature oxidation of formaldehyde in the study of 1, 3, 5-trioxane pressurized laminar flame speeds, 55th AIAA Aerospace Sciences Meeting (2017).
[28] H. Zhao, Z. Zhang, Y Rezgui, Y. Ju, Studies of high pressure 1,3-butadiene flame speeds and high temperature chemistry using hydrogen and oxygen sensitization, Energy Fuels (2018) Under review.
[29] E.J. Zhang, B. Brumfield, G. Wysocki, Hybrid faraday rotation spectrometer for sub-ppm detection of atmospheric O_2, Opt. Expr. 22 (2014) 15957–15968.
[30] http://www.reactiondesign.com/products/chemkin/chemkin-pro/
[31] C.W. Gao, J.W. Allen, W.H. Green, R.H. West, Reaction mechanism generator: automatic construction of chemical kinetic mechanisms, Comput. Phys. Commun. 203 (2016) 212–225.
[32] A.G. Dana, B. Buesser, S.S. Merchant, W.H. Green, Automated reaction mechanism generation including nitrogen as a heteroatom, Int. J. Chem. Kinet. (2018) 1–16.
[33] A.M. Dean, J.W. Bozzelli, Combustion chemistry of nitrogen, Gas-Phase Combustion Chemistry, Gardiner ed., Springer, New York, NY, 2000.
[34] P. Glarborg, J.A. Miller, R.J. Kee, Kinetic modeling and sensitivity analysis of nitrogen oxide formation in well-stirred reactors, Combust. Flame 65 (1986) 177–202.
[35] P. Glarborg, M.U. Alzueta, K. Dam-Johansen, J.A. Miller, Kinetic modeling of hydrocarbon/nitric oxide interactions in a flow reactor, Combust. Flame 115 (1998) 1–27.
[36] J.H. Bromly, F.J. Barnes, et al., Kinetic and thermodynamic sensitivity analysis of the NO-sensitised oxidation of methane, Combust. Sci. Tech. 115 (1996) 259–296.
[37] M.A. Mueller, R.A. Yetter, F.L. Dryer, Flow reactor studies and kinetic modeling of the $H_2/O_2/NO_x$ and $CO/H_2O/O_2/NO_x$ reactions, Int. J. Chem. Kinet. 31 (1999) 705–724.
[38] S.J. Klippenstein, L.B. Harding, P. Glarborg, J.A. Miller, The role of NNH in NO formation and control, Combust. Flame 158 (2011) 774–789.
[39] T. Amarno, F.L. Dryer, Effect of dimethyl ether, NO_x, and ethane on CH_4 oxidation: high pressure, intermediate-temperature experiments and modeling, Symp. (Int.) Combust. 27 (1998) 397–404.
[40] R. Atkinson, D.L. Baulch, R.A. Cox, et al., Evaluated kinetic, photochemical and heterogeneous data for atmospheric chemistry: supplement V. IUPAC subcommittee on gas kinetic data evaluation for atmospheric chemistry, J. Phys. Chem. Ref. Data 26 (1997) 521–1011.
[41] N.K. Srinivasan, M.-C. Su, J.W. Sutherland, J.V. Michael, Reflected shock tube studies of high-temperature rate constants for $OH + CH_4 \rightarrow CH_3 + H_2O$ and $CH_3 + NO_2 \rightarrow CH_3O + NO$, J. Phys. Chem. A 109 (2005) 1857–1863.
[42] K. Zhang, L. Zhang, M. Xie, L. Ye, F. Zhang, et al., An experimental and kinetic modeling study of premixed nitroethane flames at low pressure, Proc. Combust. Inst. 34 (2013) 617–624.